VANADIUM-RICH MUSCOVITE FROM AUSTRIA: CRYSTAL STRUCTURE, CHEMICAL ANALYSIS, AND SPECTROSCOPIC INVESTIGATIONS

ANDREAS ERTL[§]

Institut für Mineralogie und Kristallographie, Geozentrum, Universität Wien, Althanstraße 14, A-1090 Vienna, Austria

JOHN RAKOVAN

Department of Geology and Environmental Earth Science, Miami University, Oxford, Ohio 45056, USA

JOHN M. HUGHES

Department of Geology and Environmental Earth Science, Miami University, Oxford, Ohio 45056, USA
Department of Geology, University of Vermont, Burlington, Vermont 05405, USA

HEINZ-JÜRGEN BERNHARDT

Institut für Geologie, Mineralogie und Geophysik, Ruhr-Universität Bochum, D-44801 Bochum, Germany

GEORGE R. ROSSMAN

Division of Geological and Planetary Sciences, California Institute of Technology, Pasadena, California 91125-2500, USA

ABSTRACT

The crystal structure of a green, transparent, vanadium-rich muscovite-$2M_1$ ($V_2O_3 = 11.35$ wt.%, one of the highest amounts reported to date in muscovite) with the optimized formula $(K_{0.94}Na_{0.06})_{M2}(Al_{1.20}V^{3+}_{0.61}Mg_{0.12}Cr^{3+}_{0.07})_{T1}(Si_{1.54}Al_{0.46})_{T2}$ $(Si_{1.54}Al_{0.46})O_{10}(OH)_2$ and space group C2/c, a 5.2255(6), b 9.0704(10), c 20.0321(21) Å, β 95.773(2)°, Z = 4 has been refined to $R = 6.97\%$ for 1070 unique reflections (Mo$K\alpha$). This muscovite, which occurs in small quartz veins in graphite schist from Weinberg mountain, near the village of Amstall, Lower Austria, is distinctly low in Cr ($Cr_2O_3 \sim 1.4$ wt.%) and Mg (MgO ~ 1.1 wt.%); Fe, Mn, and Ti are below detection limit. All octahedral cations occupy the $M2$ site, and the average octahedral bond ($M2$–O) distance is 1.953 Å. Structural distortions include $\alpha = 8.89°$ and $\Delta z = 0.193$ Å, resulting in an interlayer spacing of 3.35 Å. The optical absorption spectrum of this V-rich muscovite shows absorption features at 427 and 609 nm that define a transmission window centered at 523 nm. These absorption features are consistent with those expected for V^{3+} in mica, but the 609 nm band has a slightly longer wavelength than in low-V micas.

Keywords: vanadium-bearing muscovite-$2M_1$, crystal structure, graphite schist, Amstall, Austria.

INTRODUCTION

Vanadium-bearing muscovite-$2M_1$ has been reported from several localities. Vanadium- and barium-bearing muscovite (1.48 wt.% V_2O_3, 1.95 wt.% V_2O_4, 2.39 wt.% BaO) associated with vanadium-bearing tourmaline (7.45 wt.% V_2O_3, 0.58 wt.% V_2O_4) was reported by Snetsinger (1966) from a quartz-graphite schist (Mariposa County, California, USA). In the Janggun mine area, Republic of Korea, V-bearing muscovite (5.09 wt.% V_2O_3, 0.8 wt.% Cr_2O_3) is associated with V-bearing tourmaline (*ca*. 3 wt.% V_2O_3), quartz, and graphite (Imai *et al*. 1980). Pan & Fleet (1992) described a paragenetic sequence of V-rich minerals from the Hemlo gold deposit, Ontario, Canada. Included among these are V-rich muscovite

---

§ *Corresponding author e-mail address*: andreas.ertl@a1.net

and V-bearing phlogopite. Evaluation of the reported sample chemistries (with V_2O_3 concentrations as high as 17.55%) show that their "V-rich muscovites" are in many cases roscoelite. The samples, however, are chemically zoned and occasionally tend towards a V-rich core. Vanadium-bearing muscovite (2.73 wt.% V_2O_3) having the structural formula $(K_{1.94}Na_{0.09})$ $(Al_{3.34}V^{3+}_{0.29}Mg_{0.26}Ti_{0.05}Fe_{0.04})(Si_{6.27}Al_{1.73})O_{22}(OH)_2$ and cell parameters $a = 5.19(1)$, $b = 9.05(2)$, $c = 20.23(4)$ Å, $\beta = 95.0(5)°$, associated with V- and Cr-bearing tourmaline (4.06 wt.% V_2O_3, 2.38 wt.% Cr_2O_3), graphite, and quartz, in contact-metamorphosed carbonaceous rocks from Primorye, Russia, was described by Kazachenko et al. (1993). Vanadium-rich muscovite (10.4 wt.% V_2O_3 and 3.0 wt.% Cr_2O_3) was described by Rumyantseva et al. (1984) from a metasomatic assemblage in southern Karelia, Russia. The structure of a roscoelite-1M, the vanadium-dominant analog of muscovite, from Reppia, Val Graveglia, Italy, with the formula $\sim(K_{0.99}Ba_{0.01})$ $(V_{1.70}Fe_{0.15}Mg_{0.10}Mn_{0.06}Al_{0.04})(Si_{3.15}Al_{0.85})O_{10}(OH)_2$ was described by Brigatti et al. (2003). In a study of the gold-vanadium-tellurium association at the Tuvatu gold-silver prospect, Fiji, Spry & Scherbarth (2006) showed that the most common mica at Tuvatu is roscoelite rather than V-bearing muscovite. In their analyses they reported V-rich muscovites with up to 0.7 V apfu with concomitant Al(VI) of 1 apfu.

Green V-rich muscovite from Weinberg mountain $\sim$500 m west of the village of Amstall, Lower Austria, occurs with pyrite in small quartz veins in graphite schist. Structural and chemical data and an optical absorption spectrum of green V- and Cr-bearing tourmaline with 0.85 wt.% V_2O_3 and $\sim$0.17 wt.% Cr_2O_3 from the same locality was described by Ertl et al. (2008). The core of this dravite has lattice parameters of $a = 15.984(2)$, $c = 7.222(2)$ Å, while the rim exhibits smaller lattice parameters of $a = 15.9175(5)$, $c = 7.1914(4)$ Å, mainly due to a decreasing Mg content while the V and Cr content does not change significantly. That study also confirmed that V and Cr produce similar optical absorption spectra in tourmalines. Green muscovite from this locality was first noted by Zirkl (1961). Forty years later Blass & Graf (2001) described green muscovite with a significant vanadium content in association with graphite, sillimanite, violet corundum, and pyrite.

The graphite deposit near Amstall occurs within the Bunte Series (tectonic Drosendorf unit) of the Austrian portion of the Moldanubian zone. Petrakakis et al. (1999) suggested that the Bunte Series is an old segment of crust containing a composite Proterozoic gneissic basement overlain by a late-Proterozoic to Silurian shelf and a slope-derived, pelite- and carbonate-rich, volcano-sedimentary succession. Graphite from this deposit, which is silica-rich, originated due to metamorphosis of sapropel and shows a high degree of crystallinity (Holzer 1964, Holzer & Zirkl 1962). Graphite is also a characteristic mineral in the gneisses, quartzites, and marbles of the Bunte Serie (Petrakakis et al. 1999). Pressure-temperature estimates of the metamorphic conditions, derived from typical Grt+Sil+Kfs+Bt-gneisses and some Grt+Opx-amphibolites, are 700–1100 MPa/700–800 °C and $aH_2O << 1$ (Petrakakis & Jawecki 1995, Petrakakis 1997, Petrakakis et al. 1999). This Variscan MP/HT event (around 340 Ma) was accompanied by strong decompression-induced anatexis of fertile lithologies (Petrakakis et al. 1999, Ertl et al. 2012). Although the graphite deposit is also assumed to be of Proterozoic origin, quartz-feldspar dikes (containing mica and tourmaline) within the graphite schist could be related to decompression-induced anatexis during the uplift of this unit. The quartz-feldspar dikes contain albite, oligoclase, orthoclase, quartz, muscovite (V-bearing to V-rich), sillimanite, pyrite, jarosite, natrojarosite, rutile, titanite, apatite, vivianite, xenotime-(Y), monazite-(Ce), allanite-(Ce), amstallite, siderite, calcite, and laumontite (Ertl 1995).

In this study we focus on the crystal structure of one of the most V-rich muscovites reported to date, with an average of 11.35 wt.% V_2O_3, and on the optical absorption spectra of the phase.

EXPERIMENTAL DETAILS

Crystal structure

A cleavage fragment of the V-rich muscovite crystal was mounted on a Bruker Apex CCD diffractometer equipped with graphite-monochromated Mo$K\alpha$ radiation. Refined unit-cell parameters and other crystal data are listed in Table 1. Redundant data were collected for a sphere of reciprocal space and were integrated and corrected for Lorentz and polarization factors and absorption following the multislice method using the Bruker program SAINTPLUS (Bruker AXS Inc. 2001).

The structure model was refined using starting parameters from the muscovite determination of Guggenheim et al. (1987) and the Bruker SHELXTL version 6.10 package of programs, with neutral-atom scattering factors and terms for anomalous dispersion. Refinement was performed with anisotropic thermal parameters for all atoms. In Table 2 we list the atom parameters, and in Table 3 we present selected interatomic distances.

TABLE 1. CRYSTAL DATA AND RESULTS OF STRUCTURE REFINEMENT FOR V-RICH MUSCOVITE-2M_1 FROM AMSTALL, LOWER AUSTRIA

Unit cell by least squares	$C2/c$, 7361 reflections
a (Å)	5.2255(6)
b (Å)	9.0704(10)
c (Å)	20.0321(21)
β	95.773(2)°
Frame width	0.20°
Scan time	15 s
No. of frames	4500
Crystal-to-detector distance	5 cm
Effective transmission	0.7254–1.000
R_{int} (before & after SADABS)	0.058 & 0.042
Measured reflections, full sphere to 65° 2θ	8830
Unique reflections & refined parameters to 55° 2θ	1070 & 94
$R1 = 0.0697$ for 1033 $F_o > 4\sigma(F_o)$ to 55° 2θ	
Largest difference peaks	+1.55(2), –1.17(2) e$^-$ · Å^{-3}
Goodness-of-fit	1.204

TABLE 3. SELECTED INTERATOMIC DISTANCES (Å) IN V-RICH MUSCOVITE-2M_1 FROM AMSTALL, LOWER AUSTRIA

K–O1(×2)	2.896(5)	T2–O2	1.633(6)
K–O3(×2)	2.904(6)	T2–O3	1.635(5)
K–O2(×2)	2.929(6)	T2–O5	1.649(5)
K–O3(×2)	3.239(6)	T2–O1	1.653(5)
K–O1(×2)	3.255(5)	Mean	1.643
Mean	3.045		
T1–O1	1.630(5)	M2–OH	1.936(6)
T1–O4	1.640(5)	M2–OH	1.939(6)
T1–O2	1.643(6)	M2–O5	1.955(5)
T1–O3	1.656(5)	M2–O4	1.957(5)
Mean	1.642	M2–O5	1.963(5)
		M2–O4	1.968(5)
		Mean	1.953

by EMPA and structure refinement, yielding 0.64 *apfu* by the former method and 0.58 *apfu* by the latter. The optimized formula (Wright *et al.* 2000) resulting from the chemical data and structure values is given below.

Optical spectra

A ~1 × 1 mm, 116 μm thick, green cleavage fragment of the Amstall vanadium-rich muscovite was used for the optical spectrum in the 390–1100 nm range. Spectra were obtained at about one-nm resolution with a locally built microspectrometer system consisting of a 1024-element Si diode-array detector coupled to a grating spectrometer system and *via* fiber optics to a highly modified NicPlan® infrared microscope containing a calcite polarizer. Conventional 10× objectives were used as both objective and condenser. Spectra were obtained from an approxi-

Chemical analyses

Chemical analyses (Table 4) were performed using the wavelength-dispersive spectrometers of a CAMECA SX-50 electron-microprobe at the Ruhr-University-Bochum, Germany. The microprobe was operated at an acceleration voltage of 15 kV, a sample current of 15 nA, and a beam diameter of approximately 5 μm. Natural and synthetic materials were used as standards. Excellent agreement was obtained between V analyzed

TABLE 2. TABLE OF ATOM PARAMETERS IN V-RICH MUSCOVITE-2M_1 FROM AMSTALL, LOWER AUSTRIA

Atom	x	y	z	U_{eq}	Occ.
K	0	0.0968(3)	1/4	0.0251(9)	K$_{0.970(13)}$
T1	0.0349(3)	0.42931(18)	0.36372(9)	0.0091(5)	Si$_{1.00}$
T2	0.5475(3)	0.2582(2)	0.36362(9)	0.0102(5)	Si$_{1.00}$
M2	0.7499(3)	0.0832(2)	0.49992(8)	0.0089(6)	Al$_{0.71(1)}$V$_{0.29}$
O1	0.0717(9)	0.5918(5)	0.3312(2)	0.0152(10)	O$_{1.00}$
O2	0.2561(10)	0.3168(6)	0.3406(2)	0.0188(11)	O$_{1.00}$
O3	0.7551(9)	0.3633(5)	0.3305(2)	0.0156(10)	O$_{1.00}$
O4	0.0405(9)	0.4399(5)	0.4456(2)	0.0133(10)	O$_{1.00}$
O5	0.6099(9)	0.2507(5)	0.4459(2)	0.0137(10)	O$_{1.00}$
O(H)	0.0448(10)	0.0636(6)	0.4491(3)	0.0156(10)	O$_{1.00}$
H	0.096(18)	0.126(11)	0.444(5)	0.02(3)	H$_{1.00}$

Anisotropic thermal parameters are on deposit with the V-rich muscovite .cif file.
Supplementary Data are available from the Depository of Unpublished data on the MAC website (http://mineralogicalassociation.ca/), document "V-rich mica, CM57, 1900020".

TABLE 4. COMPOSITION OF V-RICH MUSCOVITE
FROM AMSTALL, LOWER AUSTRIA (wt.%)

	Range[1]	Average[1]	V-muscovite[2]
SiO_2	43.71–44.46	44.15	44.79
Al_2O_3	25.48–26.87	26.10	26.16
Cr_2O_3	1.11–1.57	1.36	1.29
V_2O_3	10.55–11.91	11.35	11.06
MgO	0.84–1.31	1.11	1.17
Na_2O	0.26–0.35	0.31	0.45
K_2O	10.30–10.63	10.45	10.72
H_2O*	-	4.31	4.36
Sum		99.15	100.00
Ions on the basis of O = 12			
T site			
Si		3.07	3.08
Al		0.93	0.92
Sum		4.00	4.00
M site			
Al		1.21	1.20
Cr^{3+}		0.07	0.07
V^{3+}		0.64	0.61
Mg		0.11	0.12
Sum		2.03	2.00
A site			
Na		0.05	0.06
K		0.93	0.94
Sum		0.98	1.00

[1] Range and average of 11 EMP analyses. F, Fe, Mn, Ti, Ni, Ca, Ba, and REE are below detection limit.
[2] Weight percent calculated from optimal site occupancies and normalized to 100%.
* Calculated for $(OH)_2$.

mately 200×200 μm region near the rim area of the crystal. A spectrum of an irregular, 40-μm thick, olive-brown cleavage fragment of roscoelite from the Stuckslager mine, Coloma, El Dorado County, California (type locality for roscoelite), was also studied for comparison.

RESULTS AND DISCUSSION

Structure

Brigatti *et al.* (2003) published the first detailed atomic arrangement of roscoelite-1*M*, and we refer the reader to that work for a detailed examination of vanadium in the mica structure. The vanadium-rich muscovite described herein contains extensive V at the octahedral site. In contrast to the V-dominant roscoelite with its 1*M* polytype, the V-rich, Al-dominant muscovite reported here retains the common 2*M*$_1$ polytype of muscovite. We describe here the atomic

arrangement of one of the most V-rich muscovites described to date.

Dioctahedral micas typically crystallize as the 2*M*$_1$ polytype, and, as noted by Brigatti *et al.* (2003), such micas commonly contain minor atom occupancy at the *M*1 octahedral site, in addition to occupancy at *M*2, the dominant octahedral site. In the Austrian V-rich muscovite, the *M*1 site is fully vacant, as shown by final difference maps and attempts at refining any electron occupancy at the site. The electron occupancy of the *M*2 site gives excellent agreement between the chemical analysis and the refinement, confirming the putative locus of the V^{3+} substituent. The optimization (Wright *et al.* 2000) of the occupants of all the cation sites, which minimizes the differences between the chemical composition as determined by EMPA and X-ray structure refinement, yields $(K_{0.94}Na_{0.06})_{M2}$ $(Al_{1.20}V^{3+}_{0.61}Mg_{0.12}Cr^{3+}_{0.07})_{T1}(Si_{1.54}Al_{0.46})_{T2}$ $(Si_{1.54}Al_{0.46})O_{10}(OH)_2$. This V-rich muscovite is distinctly low in Cr (Cr_2O_3 ~1.4 wt.%) and Mg (MgO: ~1.1 wt.%); Fe, Mn, and Ti are below detection limit. The calculated density, from the chemical composition and the volume of the unit cell (944.65 $Å^3$), is $D_{calc} = 2.907$.

The incorporation of significant V^{3+} at the octahedral site evokes a structural response. Table 5 offers various parameters for our V-rich muscovite, roscoelite, and muscovite without vanadium substituents. Plotting $<M2–O>$ *versus* V^{3+} content yields a linear increase with V concentration, suggesting that the incorporation of the larger V^{3+} cation instead of Al in the mica structure causes an expansion of $<M2–O>$ regardless of the polytype (Fig. 1).

Brigatti *et al.* (2003) described the distortions in the dioctahedral roscoelite structure that result from the incorporation of V^{3+} at the octahedral site. They noted that the V-dominant octahedral occupants in roscoelite result in the smallest tetrahedral rotation ($\alpha = 2.3°$) and the smallest corrugation of the basal oxygen surface ($\Delta z = 0.118$ Å) known in dioctahedral micas. In our sample, these structural compensations are much larger, which indicates a greater misfit between the lateral dimensions of the sheets of tetrahedra and octahedra. The tetrahedral rotation angle is $\alpha = 8.98°$. The out-of-plane movement of bridging oxygen atoms in the basal oxygen plane result from the tetrahedral tilt of $\Delta z = 0.193$.

Figure 2 depicts the variation of tetrahedral rotation with substituent octahedral vanadium for three dioctahedral micas: muscovite, V-rich muscovite, and roscoelite. For comparison, note that roscoelite has significant amounts of octahedral iron, which is not the case for the vanadium-bearing muscovite described here. Tetrahedral rotation distorts the idealized hexagonal rings of the basal oxygen plane to ditrigonal

TABLE 5. STRUCTURAL DATA FOR V-RICH MUSCOVITE-$2M_1$ FROM AMSTALL, LOWER AUSTRIA, COMPARED TO Cr-BEARING MUSCOVITE-$2M_1$, MUSCOVITE-$2M_1$ WITH AN IDEAL END MEMBER COMPOSITION, AND ROSCOELITE-$1M$

Mica	V-rich muscovite[1]	Cr-bearing muscovite[2]	Muscovite[3]	Roscoelite[4]
Polytype	$2M_1$	$2M_1$	$2M_1$	$1M$
S.G.	$C2/c$	$C2/c$	$C2/c$	$C2/m$
a	5.2255(6)	5.206(1)	5.1579(9)	5.292(1)
b	9.0704(10)	9.040(3)	8.9505(8)	9.131(2)
c	20.0321(21)	20.058(8)	20.071(5)	10.206(3)
β (°)	95.773(2)	95.79(4)	95.75(2)	100.98(2)
M site(s)	$Al_{1.20}V^{3+}_{0.61}$ $Mg_{0.12}Cr^{3+}_{0.07}$	$Al_{1.83}Mg_{0.11}$ $Cr^{3+}_{0.11}Fe_{0.10}Ti_{0.03}$	$Al_{1.9311}Fe_{0.01}$ $Mg_{0.01}Mn_{0.01}$	$V_{1.70}Fe_{0.15}Mg_{0.10}$ $Mn_{0.06}Al_{0.04}$
<$M1$–O>	-	2.246	-	2.213
<$M2$–O>	1.953	1.937	1.916	2.020
T site(s)	$Si_{3.08}Al_{0.92}$	$Si_{3.13}Al_{0.87}$	$Si_{3.09}Al_{0.91}$	$Si_{3.15}Al_{0.85}$
<$T1$–O>	1.642	1.650	1.635	1.641*
<$T2$–O>	1.643	1.642	1.637	1.641*

Lattice parameters and bond distances in Å. S.G. = space group.
[1] This work.
[2] Cr-bearing muscovite (Nelson Anatoki River, South Island, New Zealand; $R = 3.3\%$) from Brigatti *et al.* (2001).
[3] Muscovite (Panasqueira, Portugal; at 20 °C) from Guggenheim *et al.* (1987).
[4] Roscoelite (Reppia, Val Graveglia, Italy; $R = 3.3\%$) from Brigatti *et al.* (2003).
* <T–O> distance.

symmetry, causing decreased lateral dimensions of the rings. Potassium ions sit within the ditrigonal rings of basal oxygen planes on either side of the interlayer. The decrease in the lateral dimensions of the rings affects the position of the potassium within the rings with a concomitant increase in the interlayer spacing. The interlayer spacing in the V-rich muscovite from Amstall, Lower Austria is 3.35 Å.
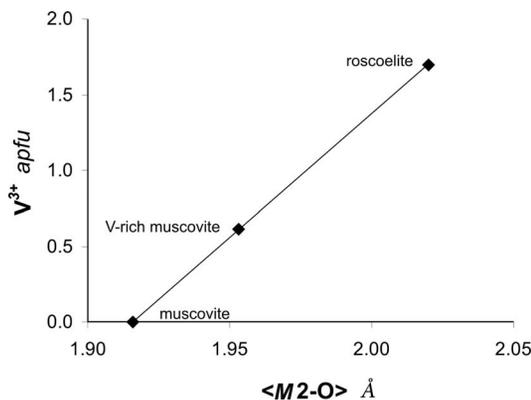

FIG. 1. Variation of <$M2$–O> with $^{[6]}V^{3+}$ content. Samples, with varying V content, are muscovite (Guggenheim *et al.* 1987), V-rich muscovite (this study), and roscoelite (Brigatti *et al.* 2003). Samples also described in Table 5.

Optical spectroscopy

The V-rich muscovite has absorption features at 427 and 609 nm that define a transmission window centered at 523 nm (Fig. 3). These absorption features are consistent with those expected for V^{3+} (Schmetzer 1982) in mica, but at a slightly longer wavelength for the 609 nm band compared to low V-content micas. The roscoelite spectrum has absorption bands at 610 and 730 nm that sit on a background that gradually rises towards shorter wavelengths (Fig. 3). The 610 nm band was observed in the reflectance spectra of other roscoelites (Schmetzer 1982, Clark *et al.* 1993) and is
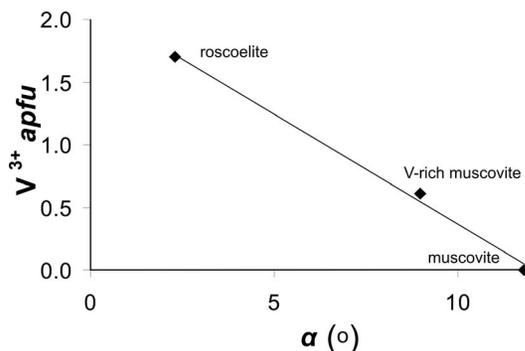

FIG. 2. Variation of tetrahedral rotation (α) with substituent V^{3+} at $M2$; samples are the same as in Figure 1.
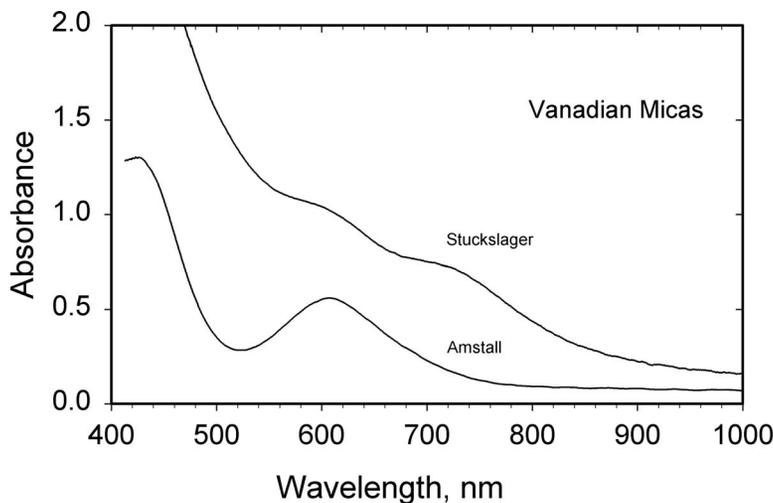
F<small>IG</small>. 3. The optical absorption spectra of two vanadium-rich micas through (001) faces of cleavage fragments. Top curve: roscoelite (GRR 1927) from the Stuckslager mine, Coloma, El Dorado County, California, USA, 0.040 mm thick. Bottom curve: muscovite from Amstall, Lower Austria, 0.368 mm thick.

a V^{3+} feature. The additional absorption band near 740 nm corresponds to a band in this region of the spectrum of micas previously attributed to either a Fe^{2+}/Fe^{3+} intervalence interaction or a V^{4+} (or VO^{2+}) feature, as reviewed in Schmetzer (1982).

Little comparative data exist on the intensities of V^{3+} bands in silicate minerals. The intensities of these bands compare favorably with the range of intensities of V^{3+} in model systems reported by Schmetzer (1982). The 610 nm band corresponds to the $^3T_1 \rightarrow {}^3T_2$ (v1) transition with intensity (ε) in the range of 4.1 to 7.8 for three model compounds, compared to 2.9 for the V^{3+}-rich muscovite. The 420 nm band corresponds to the $^3T_1 \rightarrow {}^3T_1$ (v2) transition with intensity (ε) in the range 6.6 to 10.5 for the model compounds, compared to 7.3 for the V^{3+}-rich muscovite. While these are only modestly intense bands, the intense green color of the mica is due to the high V concentration.

R<small>EFERENCES</small>

B<small>LASS</small>, G. & G<small>RAF</small>, H.-W. (2001) Vanadin enthaltender Muskovit aus der Graphitgrube am Weinberg bei Amstall. *In* Neue Mineralfunde aus Österreich L. Niederösterreich (G. Niedermayr, F. Bernhard, G. Blass, H.-P. Bojar, F. Brandstätter, K. Ettinger, H.-W. Graf, V.M.F. Hammer, B. Leikauf, H. Meditz, B. Moser, W. Postl, J. Taucher, & P. Tomazic, eds.). *Carinthia II* **191/111**, 1269.

B<small>RIGATTI</small>, M.F., G<small>ALLI</small>, E., M<small>EDICI</small>, L., P<small>OPPI</small>, L., C<small>IBIN</small>, G., M<small>ARCELLI</small>, A., & M<small>OTTANA</small>, A. (2001) Chromium-containing muscovite: crystal chemistry and XANES spectroscopy. *European Journal of Mineralogy* **13**, 377–389.

B<small>RIGATTI</small>, M.F., C<small>APRILLI</small>, E., M<small>ARCHESINI</small>, M., & P<small>OPPI</small>, L. (2003) The crystal structure of Roscoelite-1*M*. *Clays and Clay Minerals* **51**, 301–308.

B<small>RUKER</small> AXS I<small>NC</small>. (2001) *SaintPlus*. Bruker AXS Inc., Madison, Wisconsin.

C<small>LARK</small>, R.N., S<small>WAYZE</small>, G.A., G<small>ALLAGHER</small>, A.J., K<small>ING</small>, T.V.V., & C<small>ALVIN</small>, W.M. (1993) The U.S. Geological Survey, Digital Spectral Library: Version 1 (0.2 to 3.0 μm). United States Geological Survey, Open File Report 93-592.

E<small>RTL</small>, A. (1995) Elbait, Olenit, Dravit-Buergerit-Mischkristalle, Dravit, Uvit und ein neuer Al-Turmalin (?) von österreichischen Fundstellen. *Mitteilungen der*

Österreichischen Mineralogischen Gesellschaft **140**, 55–72.

ERTL, A., ROSSMAN, G.R., HUGHES, J.M., MA, C., & BRANDSTÄTTER, F. (2008) V^{3+}-bearing, Mg-rich, strongly disordered olenite from a graphite deposit near Amstall, Lower Austria: A structural, chemical and spectroscopic investigation. *Neues Jahrbuch Mineralogie Abhandlungen* **184**, 243–253.

ERTL, A., SCHUSTER, R., HUGHES, J.M., LUDWIG, T., MEYER, H.-P., FINGER, F., DYAR, M.D., RUSCHEL, K., ROSSMAN, G.R., KLÖTZLI, U., BRANDSTÄTTER, F., LENGAUER, C.L., & TILLMANNS, E. (2012) Li-bearing tourmalines in Variscan pegmatites from the Moldanubian nappes, Lower Austria. *European Journal of Mineralogy* **24**, 695–715.

GUGGENHEIM, S., CHANG, Y.H., & KOSTER VAN GROOS, A.F. (1987) Muscovite dehydroxylation: High-temperature studies. *American Mineralogist* **72**, 537–550.

HOLZER, H. (1964) Die Flinzgraphitvorkommen im außeralpinen Grundgebirge Ober- und Niederösterreichs. *Verhandlungen der Geologischen Bundesanstalt* **1964**, 360–371.

HOLZER, H. & ZIRKL, E.J. (1962) Weitere Mitteilungen über niederösterreichische Graphitlagerstätten. *Verhandlungen der Geologischen Bundes-Anstalt* **1962**, 316–330.

IMAI, H., LEE, H.K., & MACHIDA, M. (1980) Vanadium-bearing green mica from the Jangsan quartzite in Janggun mine area, Republic of Korea. *Clay Science* **5**, 221–236.

KAZACHENKO, V.T., BUTSIK, L.A., SAPIN, V.I., KITAEV, I.V., BARINOV, N.N., & NARNOV, G.A. (1993) Vanadian-chromian tourmaline and vanadian muscovite in contact-metamorphosed carbonaceous rocks, Primorye, Russia. *Canadian Mineralogist* **31**, 347–356.

PAN, Y. & FLEET, M.E. (1992) Mineral chemistry and geochemistry of vanadian silicates in the Hemlo gold deposit, Ontario, Canada. *Contributions to Mineralogy and Petrology* **109**, 511–525.

PETRAKAKIS, K. (1997) Evolution of Moldanubian rocks in Austria: Review and synthesis. *Journal of Metamorphic Geology* **15**, 203–222.

PETRAKAKIS, K. & JAWECKI, C. (1995) High-grade metamorphism and retrogression of Moldanubian granulites, Austria. *European Journal of Mineralogy* **7**, 1183–1203.

PETRAKAKIS, K., KLÖTZLI, U., & RICHTER, W. (1999) Excursion to the Austrian part of Moldanubia. *European Journal of Mineralogy Beihefte* **11**, 61–90.

RUMYANTSEVA, E.V., MISHCHENKO, K.S., & KALINICHEVA, L.I. (1984) Tainiolite and chrome-vanadium micas in metasomatites of Karelia. *Zapiski Vsesojuznogo Mineralogieskogo Obščestva* **113(1)**, 67–75 (in Russian).

SCHMETZER, K. (1982) Absorption spectroscopy and color of V^{3+}-bearing natural oxides and silicates - a contribution to the crystal chemistry of vanadium. *Neues Jahrbuch Mineralogie Abhandlungen* **144**, 73–106.

SNETSINGER, K.G. (1966) Barium-vanadium muscovite and vanadium tourmaline from Mariposa County, California. *American Mineralogist* **51**, 1623–1639.

SPRY, P.G. & SCHERBARTH, N.L. (2006) The gold–vanadium–tellurium association at the Tuvatu gold–silver prospect, Fiji: conditions of ore deposition. *Mineralogy and Petrology* **87**, 171–186.

WRIGHT, S.E., FOLEY, J.A., & HUGHES, J.M. (2000) Optimization of site-occupancies in minerals using quadratic programming. *American Mineralogist* **85**, 524–531.

ZIRKL, E.J. (1961) Vorläufiger Bericht über die mineralogischen Untersuchungen einiger Graphitvorkommen aus dem niederösterreichischen Waldviertel. *Verhandlungen der Geologischen Bundesanstalt* **1961**, 99–101.